J. Plasma Physics (2006), *vol.* 72, *part* 6, *pp.* 1291–1294.
doi:10.1017/S0022377806005575 Printed in the United Kingdom

Ionization dynamics in high-power laser–matter interaction

T. MASAKI[1] and Y. KISHIMOTO[1,2]

[1]Graduate School of Energy Science, Kyoto University, Gokasyo, Uji, Kyoto 611-0011, Japan

[2]Naka Fusion Research Establishment, JAERI, Mukoyama 801, Naka, Ibaraki 311-0193, Japan

(Received August 2005 and accepted 14 December 2005)

Abstract. By using a particle code including atomic and relaxation processes, we investigated the ionization dynamics of a carbon film irradiated by an intense laser pulse. We found two types of ionization dynamics, namely, a fast time scale convective propagation of the ionization front with C^{4+} triggered by induced plasma waves, and a slow front with C^{5+} and C^{6+} triggered by heated electrons due to non-local thermal conduction. Thus, ionization dynamics in solids are found to evolve through multiple stages.

1. Introduction

Development of ultra-short, high-power lasers opens up various innovative applications, such as a fast-ignition-based laser fusion, compact electron and ion accelerators, high-intensity short pulse X-ray and neutron sources, etc. [1]. Many computational works have been done to analyze such laser–matter interactions, but most of them made an *a priori* assumption of an ideal plasma as the initial condition. However, for applications utilizing relatively high-Z materials, complex atomic processes, such as ionization and recombination, and also relaxation processes among charged particles, may play an important role in determining the evolution of the interaction.

In order to study such complex physical processes, we have developed an extended particle-based integrated code EPIC3D which includes such atomic and relaxation processes. By using the code, we investigated the ionization dynamics of a carbon thin film irradiated by a short-pulse high-power laser. We found prominent ionization dynamics which evolve transiently in the solid through multiple stages. Specifically, it is found that Cherenkov-type plasma waves and/or wake emissions induced by fast electrons leads to tunneling field ionizations in the solid.

2. Model of relaxation and atomic processes in particle code

In order to investigate the detailed ionization dynamics in a solid thin film, here we have developed a particle-based integrated code EPIC3D by incorporating collisional relaxation and ionization processes of charged particles. The collisional relaxation process is taken into account by the Monte Carlo technique via successive binary collisions of particle pairs, which precisely conserves the momentum and

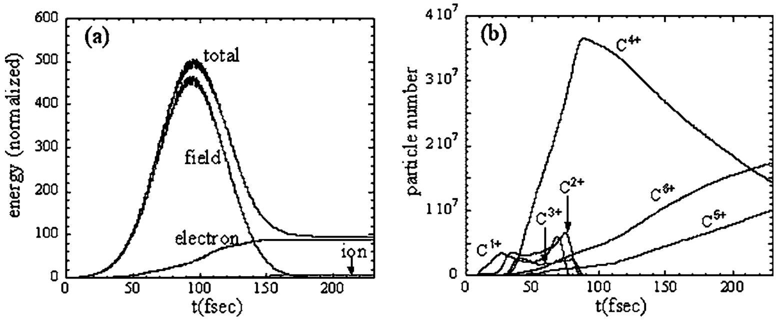

Figure 1. (a) Time histories of electron, ion and field energy. (b) Time histories of ion abundance with charge state C^{q+}.

energy in the relativistic regime [2, 3]. Therefore, the non-local heat transport, which is crucial to determine the kinetic structure in the solid, can be treated. The ionization effects are also taken into account by the Monte Carlo technique. For field ionization, the rate is calculated using the cycle-averaged Ammosov–Delone–Krainov (ADK) formula [5]. For electron impact ionization, the cross section is calculated using the Binary-encounter-Bethe (BEB) model [6] for every electron–ion pair inside the computational mesh.

3. Ionization dynamics in laser–thin film interaction

Using a two-dimensional version of the EPIC3D, we studied the interaction between solid carbon film and short pulse laser with the focused peak intensity of $5.1 \times 10^{19}\,\mathrm{W\,cm^{-2}}$ (normalized amplitude $a_0 = 5$). Here the wavelength and pulse width of the laser are $0.82\,\mu$m and 100 fs, respectively. The system size is $L_x = 13.12\,\mu$m and $L_y = 1.64\,\mu$m, and the thickness of the film is $8.2\,\mu$m. The p-polarized laser pulse is emitted in the x-direction from the antenna placed at $x = -2.56\,\mu$m.

The time histories of the mean electron and ion energies as well as the field energy are shown in Fig. 1(a). The corresponding time histories of the ion abundance with the charge state C^{q+} is shown in Fig. 1(b). As seen in Fig. 1(b), as the laser pulse hits the film, ionization is successively triggered from C^{1+} to a higher charge state. Interestingly, the number of the charge state $q = 4$ almost linearly increases with time. Furthermore, the number of C^{5+} and C^{6+} gradually increase even after the direct interaction with the laser pulse has ceased.

Figure 2 shows the normalized ion charge density profile ($\Sigma_j q_j n_j / e n_0$) at different time scales, i.e. Fig. 2(a) shows profiles from 30.8 to 82.1 fs and Fig. 2(b) shows those from 82.1 to 225.1 fs. Here, n_j and q_j ($= je$) represent the ion density and charge of the charge state j, and n_0 is the solid carbon density. A localized high-density distribution is seen in a narrow region near the surface. From this region, ionization proceeds inside and a hump with a steep density gradient is formed in the front. Around the peak of the laser pulse ($t = 82.1$ fs), the front reaches to the rear side, leading to a flat density profile over the whole carbon film. The density in the flat region corresponds to the density at which the carbon is thoroughly ionized to C^{4+}. Hence, it is concluded that the propagation observed in Fig. 2(a) corresponds to an ionization front to the charge state $q = 4$. The speed of the front is high, estimated as $1.3 \times 10^8\,\mathrm{m\,sec^{-1}}$. The linear increase of C^{4+} with time as seen in Fig. 1(b) is ascribed to this convective propagation of the front.

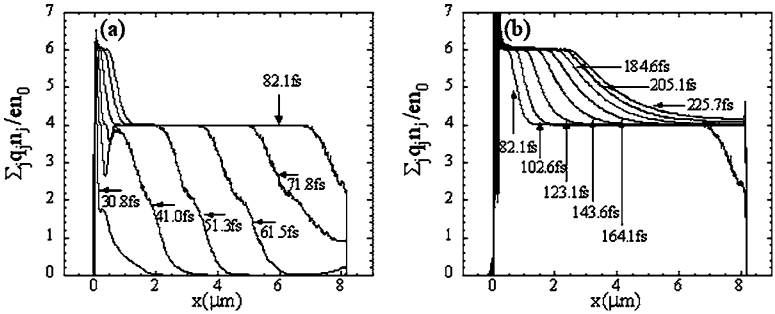

Figure 2. Ion charge density distributions (a) from 30.8 to 82.1 fs and (b) from 82.1 to 205.1 fs. All charges are summed up.

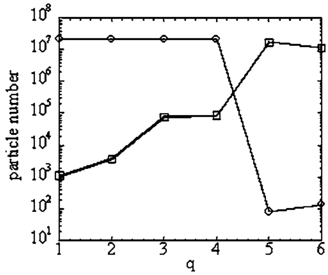

Figure 3. Statistics of ionization processes.

Followed by the propagation of C^{4+}, ionizations to higher charge states, i.e. $q = 5$ and $q = 6$, are triggered as seen in Fig. 2(b), and the front also starts to convectively propagate from the surface region to the inside. The speed of this front is around $1.7 \times 10^7\,\mathrm{m\,sec^{-1}}$, which is one order magnitude slower than that for C^{4+}. This suggests that the ionization mechanism is different. It is also noted that a diffusive nature is blended in the propagation of C^{6+} especially in the downstream region on the rear side.

In order to study the ionization mechanism in two different regimes, we investigated the number of electrons produced by field ionization and by electron impact in each electronic state of the atom in Fig. 3. It is clearly seen that ionization up to the charge state $q = 4$ is produced by the field ionization, whereas ionization to the charge states $q = 5$ and 6 results from the electron impact. Therefore, it is concluded that the fast convective propagation is triggered by the field, whereas the subsequent slow propagation is triggered by the electron impact.

Figure 4 shows the spatial distributions of (a) the normalized ion charge density $(\Sigma_j q_j n_j / e n_0)$ and (b) the longitudinal electric field (E_x) at 61.5 fs. In Fig. 4(a), complex corrugated structures of charge density are seen in $3.5\,\mu\mathrm{m} < x < 5.5\,\mu\mathrm{m}$, which corresponds to the ionization front with a steep density gradient. As also seen in Fig. 4(b), micro-scale electric fields that are oscillating similar to those in turbulence are excited from the front region towards the upstream direction. The amplitude of the waves is of the order of $10^9\,\mathrm{V\,cm^{-1}}$, which is near the threshold value to ionizations from C^{2+} to C^{3+} and, subsequently, C^{4+}. We also investigated the characteristic of the waves and found that the relation $\omega \sim k_x v_e$ is approximately satisfied, where $k_x \sim 9 \times 10^5\,\mathrm{cm^{-1}}$ is the typical wave number, $\omega \sim 2.7 \times 10^{16}\,\mathrm{s^{-1}}$ is the plasma

https://doi.org/10.1017/S0022377806005575 Published online by Cambridge University Press

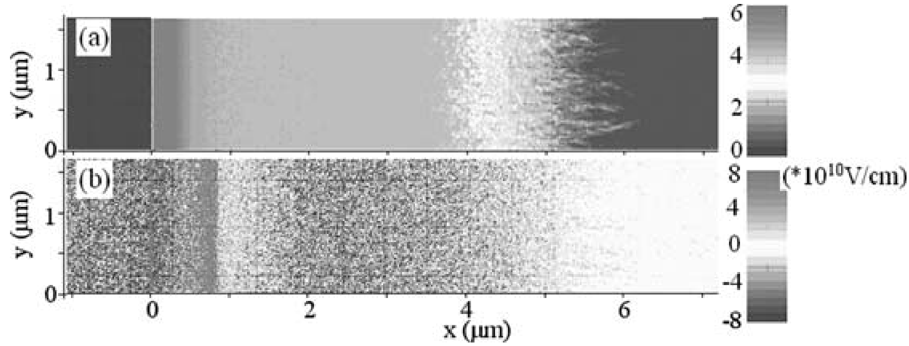

Figure 4. (a) Ion charge density, (b) longitudinal electric field (E_x) at $t = 61.5$ fs.

frequency for C^{2+} plasma, and $v_e \sim 3 \times 10^{10}$ cm s^{-1} is the typical velocity of fast electrons produced near the surface. This suggests that the Cherenkov-type plasma waves or wake emissions are the origin of the field ionization [7].

Furthermore, a quasi-stationary positive electric field was observed at $x \sim 0.8\,\mu$m. This corresponds to a thermal electric field revealed near the front due to electron non-local heat transport associated with a steep pressure gradient [8]. Namely, energetic tail electrons heated by non-local thermal conduction lead to ionization to C^{5+} and, finally, C^{6+} through impacts and trigger the propagations.

4. Conclusions

We have investigated the ionization dynamics of a thin carbon film irradiated by an intense laser pulse. We found a prominent ionization dynamics which evolves through multiple time scales. These are a fast convective propagation triggered by tunneling field ionization and a slow propagation triggered by heated electrons due to non-local thermal conduction. These ionization dynamics are important for studying various applications using laser–matter interaction.

References

[1] Tabak, M. et al. 2005 Review of progress in fast ignition. *Phys. Plasmas* **12**, 057305.

[2] Takizuka, T. and Abe, H. 1977 A binary collision model for plasma simulation with a particle code. *J. Comput. Phys.* **25**, 205–219.

[3] Sentoku, Y., Mima, K., Kishimoto, Y. and Honda, M. 1998 Effects of relativistic binary collisions on PIC simulation of laser plasmas. *J. Phys. Soc. Japan* **67**, 4048–4088.

[4] Kato, S., Kishimoto. Y., and Koga J. 1997 Convective amplification of wake field due to self-modulation of a laser pulse induced by field ionization. *Phys. Plasmas* **5**, 292–299.

[5] Ammosov, M. V., Delone, N. B. and Krainov, V. V. 1986 Tunnel ionization of complex atoms and of atomic ions in an alternating electromagnetic field. *Sov. Phys.–JETP* **64**, 1191–1194.

[6] Kim, K. and Rudd M. E. 1994 Binary-encounter-dipole model for electron-impact ionization. *Phys. Rev. A* **50**, 3954–3967.

[7] Ichimaru, S. 1973 In: *Basic Principle of Plasma Physics*, p. 62. New York: Benjamin.

[8] Kishimoto, Y., Mima, K., and Haines, M. G. 1988 An extension of Spitzer–Harm theory on thermal transport to steep temperature gradient case. II. Integral representation. *J. Phys. Soc. Japan* **57**, 1972–1986.

https://doi.org/10.1017/S0022377806005575 Published online by Cambridge University Press